CRYSTAL GROWTH & DESIGN
2009
VOL. 9, NO. 2
1216–1218

Formation of Spatially Addressed Ga(As)Sb Quantum Rings on GaAs(001) Substrates by Droplet Epitaxy

Pablo Alonso-González,* Luisa González, David Fuster, Yolanda González, Alfonso G. Taboada, and José María Ripalda

Instituto de Microelectrónica de Madrid (IMM-CNM, CSIC), Isaac Newton, 8 Tres Cantos, Madrid 28760 Spain

Ana M. Beltrán, David L. Sales, Teresa Ben, and Sergio I. Molina

Departamento de Ciencia de los Materiales e I.M. y Q.I., Universidad de Cádiz, 11510 Puerto Real, Cádiz, Spain

Received October 21, 2008; Revised Manuscript Received November 7, 2008

ABSTRACT: In this work we report on the ability to form low density Ga(As)Sb quantum ring-shaped nanostructures (Q-rings) on GaAs(001) substrates by the droplet epitaxy technique. The Q-rings are formed by crystallization of Ga droplets under antimony flux. After being capped by a GaAs layer, these nanostructures show surface mounding features that are correlated with the buried nanostructures, as demonstrated by TEM analysis, permitting an easy surface location of the optically active Q-rings.

Introduction

The formation of low density semiconductor nanostructures is presently receiving much attention due to their possible integration as single active elements in different quantum optoelectronic devices.[1−3] In this direction, the technology used must fulfill some requirements in the control of size, shape, and location of the used nanostructures.[3,4] Different strategies have been followed to overcome the inherent randomness of the Stranski-Krastanow (SK) self-assembling process on the growth of quantum structures with control of all these properties. One common approach is the use of prepatterned substrates,[5−8] which has yielded good results on the growth selectivity and photoluminescence (PL) emission of single QD.[5−7] Another approach based on the droplet epitaxy growth technique[9] has recently emerged as an optimal strategy for obtaining different nanostructures complexes.[10−14] In particular, the growth of ring-like structures with optimal uniformity and rotational symmetry have been obtained and well studied in the GaAs/AlGaAs system.[10,11] Nanostructures with a ring-like shape were originally obtained in the InAs/GaAs system by molecular beam epitaxy (MBE).[15] The formation[16] and physical properties of these Q-rings have been extensively studied in the past. Because of their specific geometry, these nanostructures show unique electronic properties that have permitted the observation of quantum mechanics interference effects such as Aharonov-Bohm-like oscillations.[17] More recently, Q-ring formation by self-assembling processes in the GaSb/GaAs system has also been reported.[18]

Related to surface location of buried nanostructures, some results have been reported using stacked structures of QD[1] and, more recently, by evaluating the morphology of the top surface once a single layer of QD was capped.[3]

In this paper, we extend the droplet epitaxy technique to the formation of low density Ga(As)Sb Q-rings by Ga droplet crystallization under Sb flux. When these nanostructures are capped by a GaAs layer, we observe surface mounds that are univocally correlated with the buried nanostructures, permitting their useful direct surface location for further technological processes. The photoluminescence of these nanostructures show characteristic features of a type II band alignment. Also, these type II Q-rings present a larger diameter than those described in the literature for InAs self-assembled Q-rings,[16] making them good candidates for the observation of Aharonov-Bohm effects at relatively low magnetic fields.

Experimental Procedures

The experimental procedure starts growing a 0.5 μm thick undoped GaAs buffer layer at a growth rate rg = 0.5 monolayers per second (ML/s), As_4 beam equivalent pressure (BEP) of 2×10^{-6} Torr and substrate temperature $T_s = 580$ °C on GaAs (001) substrates by MBE. The root-mean-square (rms) roughness of this surface is typically 0.24 nm. T_s is then decreased to 500 °C and the Ga shutter opened during 7 s, at an equivalent GaAs rate of 0.5 ML/s, for Ga droplet formation. Droplet crystallization occurs during a 60 s Sb exposure at BEP (Sb) of 3×10^{-7} Torr and $T_s = 200$ °C.

For PL characterization, another sample was grown with nanostructures capped by a 47 nm thick GaAs layer deposited at rg = 0.5 ML/s. The initial 60 ML (17 nm) of GaAs were grown at $T_s = 450$ °C with a BEP (As_2) of 2×10^{-6} Torr by atomic layer molecular beam epitaxy technique (ALMBE).[19] The cap layer is completed by MBE growth at $T_s = 580$ °C and As_4 BEP of 2×10^{-6} Torr. For morphological studies, an additional layer of Q-rings was grown on this surface, using the above-described conditions.

The surface morphology of the as grown samples was characterized by atomic force microscopy (AFM) in tapping mode. PL measurements at $T = 28$ K were made with a standard setup using a frequency-doubled Nd:YAG laser ($\lambda_{exc} = 532$nm) as excitation source, with a spot diameter of approximately 200 μm.

Cross sectional specimens for transmission electron microscopy (TEM) were produced by mechanical thinning and ion milling. Images have been acquired at 120 kV with a JEOL 1200EX transmission electron microscope, mainly using 002 dark field reflection, whose intensity contrast is related to chemical changes.

Results and Discussion

Figure 1a shows the AFM topography of a sample with a single uncapped layer of nanostructures. We observe ringlike structures with a density $\rho = 2 \times 10^8$ cm^{-2}; the average dimensions, measured with respect to the flat surface, are 2.9 ± 0.4 nm in contour height and 128 ± 5 nm and 176 ± 5 nm

* To whom correspondence should be addressed. E-mail: palonso@imm.cnm.csic.es.

10.1021/cg801186w CCC: $40.75 © 2009 American Chemical Society
Published on Web 12/19/2008

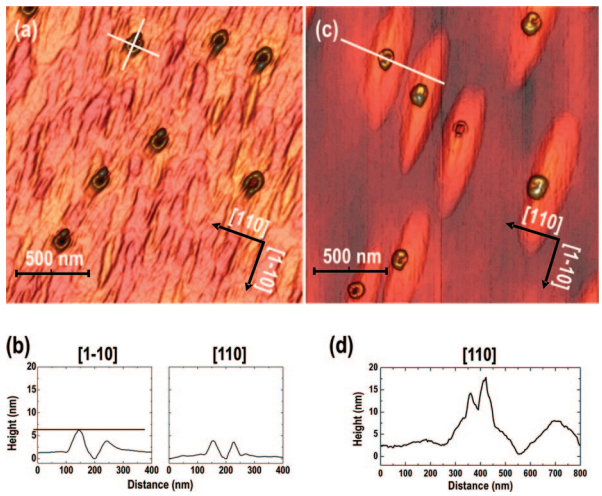

Figure 1. (a) 2 × 2 μm^2 3D AFM micrograph showing Ga(As)Sb nanostructures grown by the droplet epitaxy technique. (b) Profiles along the [1$\bar{1}$0] and [110] directions of uncapped Q-rings. (c) 2 × 2 μm^2 AFM image of Ga(As)Sb nanostructures grown on a 47 nm thick GaAs layer that caps the nanostructures shown on (a). (d) Profile along the [110] direction of a Q-ring nucleated on top of a mound.

in outside diameter along the [110] and [1$\bar{1}$0] directions, respectively. At their center, a hole with an average depth of 1.0 ± 0.3 nm is also observed (Figure 1b).

A side lobe with an average height of 5.9 ± 0.4 nm is always formed at the edge of each ring as can be noticed in the AFM profiles of Figure 1b. These side lobes systematically appear along the [1$\bar{1}$0] direction. A similar observation has been made for InAs Q-rings, but in the later case, two symmetrical lobes along the [1$\bar{1}$0] direction are observed for each ring.[17] These morphological features are expected to strongly influence the optical properties of the nanostructures as vertical confinement, together with composition, are the key factors that determine the emission wavelength.

The AFM topography in Figure 1c shows Q-rings formed on the 47 nm thick cap layer surface. We observe that Q-rings are nucleated on top of elongated structures formed on an otherwise flat GaAs surface (rms roughness of 0.4 nm). The elongated structures (mounds) appear with exactly the same density measured for the uncapped Q-rings. Their typical dimensions are 900 nm along the [1$\bar{1}$0] direction, 200 nm along the [110] direction and 9 nm in height (Figure 1d). Similar mounds have been reported for layers grown on top of both strained and unstrained nanostructures.[3,20,21] As it is well-known, these mounds result from the incomplete planarization of the initial condition of the surface during further growth.[22,23] The Q-rings formed on the mounds are 124 ± 11 nm in outside diameter along [110], with holes 9.3 ± 3.5 nm in depth referring to the highest point of the ring.

As is clearly observed, the nanostructures nucleated on the flat GaAs (001) surface (Figure 1a,b) present superior uniformity in size and shape in comparison with those nucleated on top of mounds (Figure 1c,d). The formation of GaAs rings using droplet epitaxy at a high substrate temperature (T_s = 500 °C) has been explained on the basis of Ga droplets reacting chemically with the GaAs substrate because of an imbalance of As chemical potential.[12] In our particular growth process, under antimony atmosphere, the crystallization will be more complex, involving not only As incorporation in the Ga droplets from the GaAs matrix, but also incorporation of Sb and the accompanying strain due to lattice mismatch. In the case of

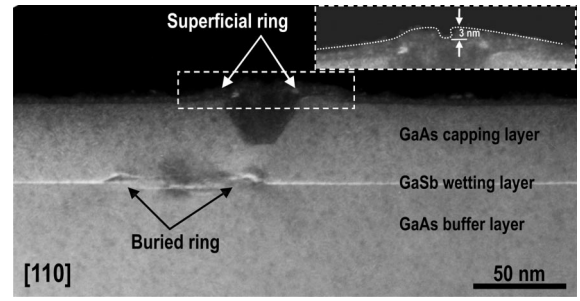

Figure 2. 002 dark field cross sectional TEM micrograph showing a buried Ga(As)Sb Q-ring correlated with a superficial ring, obtained close to the [110] zone axis. The inset in the figure shows the 3 nm deep hole of the Q-ring at the surface, which corresponds with the one measured with AFM.

nanostructures grown on top of the mounds, besides the above-mentioned effects, the nonuniform surface stress profile due to the buried nanostructures has to be taken into account. This additional stress contribution may affect the kinetics of the process, leading to dispersion in the Q-rings shape (Figure 1c).

The nucleation of a Q-ring on top of each mound, and the mounds themselves, suggests the existence of a buried nanostructure underneath. An univocal correspondence between the surface mounds and the buried Q-rings would lead to a selective formation of nanostructures on top of these, as the strain induced by the capped nanostructures would create there a local energy minima for Sb atoms incorporation.[24]

Besides the results obtained by AFM (Figure 1c), our TEM results illustrate this effect. Figure 2 depicts a 002 dark field cross section image obtained close to [110] zone axis of a buried Q-ring correlated with a ring on surface. This correlation is systematically found for other Q-rings analyzed in the electron transparent area of the TEM sample. A shift of 43 nm along [1$\bar{1}$0] is measured between both rings (buried and superficial). The superficial valley at the surface (see inset of Figure 2) corresponds with that measured by AFM. The dark contrast with a trapezoidal shape observed in the nanostructure at the surface would be related to the central opening of the original nanohole formed during the strain-mediated crystallization under Sb. As previous reported work[21] indicates, these TEM results reflect the complex droplet crystallization process, which in our case also incorporates the effect of strain. A deeper study is needed to fully understand the observed TEM images. However, it seems rather clear that the hole of the superficial Q-ring is located above one of the lobes of the buried one (probably the higher lobe), indicating that below each mound there is one Q-ring.

The photoluminescence (PL) signal of the buried nanostructures is shown in Figure 3a (blue line) together with that of a reference sample (black line). The reference sample was grown reproducing the same experimental conditions (Sb pressure, substrate temperature, and growth interruptions) except for the Ga deposition that was restricted to 1 ML to avoid formation of droplets. At high energies, the emission from the substrate and a peak at 1.45 eV possibly due to the emission from a Ga(As)Sb wetting layer is observed in both samples.[25] A broad PL band at 1.05 eV is observed only in the sample with nanostructures. Owing the low density of nanostructures and the type II band alignment between GaAs and GaSb, a low PL intensity is expected. In terms of wavelength and PL width, this emission is similar to that reported from GaSb quantum dots in a GaAs matrix.[26,27] A full width at half-maximum

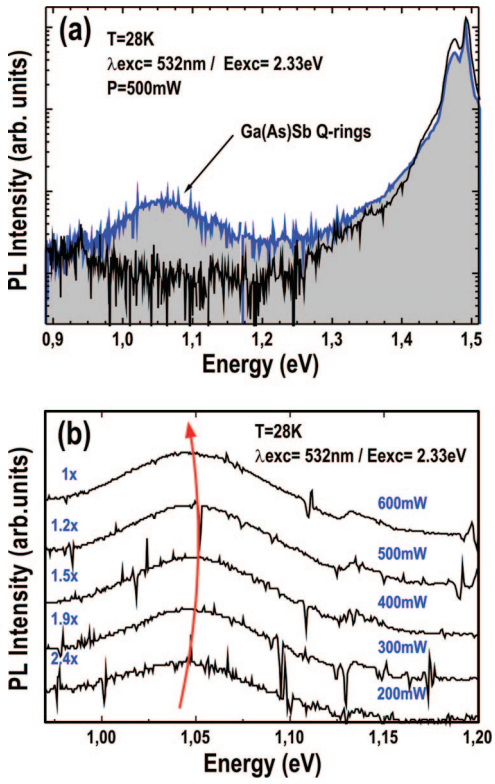

Figure 3. Photoluminescence (PL) spectra from the Ga(As)Sb Q-ring-like nanostructures sample (blue line) as compared to a reference sample that does not contain nanostructures (black line). The nanostructures show a broad PL emission centered at 1.05 eV. (b) Evolution with the excitation power.

(fwhm) of 104 meV for this band at an excitation power of 500 mW is obtained by fitting the PL signal with a Gaussian line-shape.

Figure 3b shows the PL emission of the nanostructures as a function of the excitation power. The curved arrow drawn on this figure is a guide to the eye to show the behavior of the peak energy, obtained by a Gaussian fit, with increasing excitation power. At the lower excitation powers used in this experiment (< 400 mW), a 7 meV blue shift is observed. This blue shift together with the measured cube root dependence of the PL peak emission energy with the excitation laser intensity (not shown) clearly points out the type II band alignment of the nanostructures.[24,25] For excitation powers above 400 mW, a red shift of the PL peak energy is observed, most likely due to sample heating.

Conclusions

In conclusion, we have extended the droplet epitaxy technique to the formation of low density type II Ga(As)Sb Q-rings on GaAs (001) surfaces. Moreover, the capping process results in the formation of surface mounds correlated with the buried nanostructures, as demonstrated by TEM analysis, permitting a very useful surface identification of the optically active Q-rings. This result might be highly relevant for the fabrication of quantum optics devices, since it will allow defining the exact active nanostructure location with a simple and nondestructive surface topography measurement.

Acknowledgment. The authors gratefully acknowledge the financial support by the Spanish MEC (TEC-2005-05781-C03-01/-03, NAN2004-09109-C04-01/-03, Consolider-QOIT CSD-2006-0019), CAM (S-505/ESP/000200), JA (TEP383) and by the European Commission through SANDIE Network of Excellence (No. NMP4-CT-2004-500101). P.A.G. thanks the I3P program.

References

(1) Badolato, A.; Hennessy, K.; Atatüre, M.; Dreiser, J.; Hu, E.; Petroff, P. M.; Imamouglu, A. *Science* **2005**, *308*, 1158.
(2) Stevenson, R. M.; Young, R. J.; Atkinson, P.; Cooper, K.; Ritchie, D. A.; Shields, A. J. *Nature* **2006**, *439*, 179.
(3) Hennessy, K.; Badolato, A.; Wigner, M.; Gerace, D.; Atatüre, M.; Gulde, S.; Fält, D.; Hu, E. L.; Imamoglu, A. *Nature* **2007**, *445*, 896.
(4) Vahala, K. J. *Nature* **2003**, *424*, 839.
(5) Song, H. Z.; Usuki, T.; Hirose, S.; Takemoto, K.; Nakata, Y.; Yokoyama, N.; Sakuma, Y. *Appl. Phys. Lett.* **2005**, *86*, 113118.
(6) Kiravittaya, S.; Benyoucef, M.; Zapf-Gottwick, R.; Rastelli, A.; Schmidt, O. G. *Appl. Phys. Lett.* **2006**, *89*, 233102.
(7) Atkinson, P.; Ward, M. B.; Bremner, S. P.; Anderson, D.; Farrow, T.; Jones, G. A. C.; Shields, A. J.; Ritchie, D. A. *Jpn. J. Appl. Phys.* **2006**, 2519 Part 1 45.
(8) Alonso-González, P.; González, L.; González, Y.; Fuster, D.; Fernández-Martínez, I.; Martín- Sánchez, J.; Abelmann, L. *Nanotechnology.* **2007**, *18*, 355302.
(9) Mano, T.; Watanabe, K.; Tsukamoto, S.; Fujioka, H.; Oshima, M.; Koguchi, N. *J. Cryst. Growth* **2000**, *209*, 504.
(10) Mano, T.; Kuroda, T.; Sanguinetti, S.; Ochiai, T.; Tateno, T.; Kim, J.; Noda, T.; Kawabe, M.; Sakoda, K.; Kido, G.; Koguchi, N. *Nano Lett.* **2005**, *5*, 425.
(11) Lee, J. H.; Wang, Zh. M.; Abuwaar, Z. Y.; Strom, N. W.; Salamo, G. J. *Nanotechnology* **2006**, *17*, 3973.
(12) Wang, Zh. M.; Liang, B. L.; Sablon, K. A; Salamo, G. J. *Appl. Phys. Lett.* **2007**, *90*, 113120.
(13) Lee, J. H.; Wang, Zh. M.; Ware, M. E.; Wijesundara, K. C.; Garrido, M.; Stinaff, E. A.; Salamo, G. J. *Cryst. Growth Des.* **2008**, *8*, 1945–1951.
(14) Alonso-González, P.; Alén, B.; Fuster, D.; González, Y.; González, L.; Martínez-Pastor, J. *Appl. Phys. Lett.* **2007**, *91*, 163104.
(15) García, J. M.; Medeiros-Ribeiro, G.; Schmidt, K.; Ngo, T.; Feng, J. L.; Lorke, A.; Kotthaus, J.; Petroff, P. M. *Appl. Phys. Lett.* **1997**, *71*, 2014.
(16) Granados, D.; García, J. M. *Appl. Phys. Lett.* **2003**, *82*, 2401.
(17) Kleemans, N. A. J. M.; Bominaar-Silkens, I. M. A.; Fomin, V. M.; Gladilin, V. N.; Granados, D.; Taboada, A. G.; García, J. M.; Offermans, P.; Zeitler, U.; Christianen, P. C. M.; Maan, J. C.; Devreese, J. T.; Koenraad, P. M. *Phys. Rev. Lett.* **2007**, *99*, 146808.
(18) Timm, R.; Lenz, A.; Eisele, H.; Ivanova, L.; Dähne, M.; Balakrishnan, G.; Huffaker, D. L.; Farrer, I.; Ritchie, D. A. *J. Vac. Sci. Technol. B* **2008**, *26*, 1492.
(19) Briones, F.; González, L.; Ruiz, A. *Appl. Phys. A: Solids Surf.* **1989**, *49*, 729.
(20) Atkinson, P.; Kiravittaya, S.; Benyoucef, M.; Rastelli, A.; Schmidt, O. G. *Appl. Phys. Lett.* **2008**, *93*, 101908.
(21) Wang, Zh. M.; Mazur, Yu. I.; Sablon, K. A; Mishima, T. D.; Johnson, M. B.; Salamo, G. J. *Phys. Status Solidi* **2008**, *6*, 281.
(22) Ballestad, A.; Ruck, B. J.; Adamcyk, M.; Pinnington, T.; Tiedje, T. *Phys. Rev. Lett.* **2001**, *86*, 2377.
(23) Constantini, G.; Rastelli, A.; Manzano, C.; Acosta-Diaz, P.; Songmuang, R.; Katsaros, G.; Schmidt, O. G.; Kern, K. *Phys. Rev. Lett.* **2006**, *96*, 226106.
(24) Yang, B.; Liu, F.; Lagally, M. G. *Phys. Rev. Lett.* **2004**, *92*, 025502.
(25) Lo, M. C.; Huang, S. J.; Lee, C. P.; Lin, S. D.; Yen, S. T. *Appl. Phys. Lett.* **2007**, *90*, 243102.
(26) Alonso-Álvarez, D.; Alén, B.; García, J. M.; Ripalda, J. M. *Appl. Phys. Lett.* **2007**, *91*, 263103.
(27) Suzuki, R.; Hogg, A.; Arakawa, Y. *J. Appl. Phys.* **1999**, *85*, 8349.

CG801186W